Bull. Chem. Soc. Jpn., 70, 2357—2367 (1997)

Headline Articles

Hydrophobic Hydration Structures of Tris(1,10-phenanthroline)metal and Tris(2,2′-bipyridine)metal Complex Ions and Effect of the Ionic Charge. X-Ray Diffraction Study with Isomorphous Substitution

Haruhiko Yokoyama,* Kazuteru Shinozaki, Shin Hattori, and Fumiyo Miyazaki

Department of Chemistry, Yokohama City University, Seto, Kanazawa-ku, Yokohama 236

(Received May 14, 1997)

X-Ray diffraction measurements have been made for aqueous solutions of sulfates or chlorides of $[Ru(phen)_3]^{2+}$, $[Ni(phen)_3]^{2+}$, $[Ru(bpy)_3]^{2+}$, $[Ni(bpy)_3]^{2+}$, $[Rh(bpy)_3]^{3+}$, and $[Cr(bpy)_3]^{3+}$ (phen = 1,10-phenanthroline, bpy = 2,2′-bipyridine). Radial distribution functions for the metal interactions were obtained by the isomorphous substitution between ruthenium(II) and nickel(II) complexes or between rhodium(III) and chromium(III) complexes. Metal–nitrogen and metal–carbon distances within the complex ions in solution were essentially in agreement with those in the crystals. Regarding the divalent metal complexes, about two water molecules seemed to exist at a distance of 3.5—3.6 Å (1 Å = 10^{-10} m) from the central metal atom and 10—11 water molecules existed in the region of 5.3 to 6.3 Å, probably in the vicinity of peripheral hollows along the C_3 axis of the complex. Further, large broad peaks with high electron density were observed around 7.7 and 11.2 Å for the $[Ru(bpy)_3]^{2+}$ ion and around 8.0 and 11.5 Å for the $[Ru(phen)_3]^{2+}$ ion, almost independent of salt concentration and kinds of counter ions. These were attributed to the hydrophobic hydration shells having the hydrogen-bonded network structure. The hydration structure of the trivalent metal complexes was significantly different from that observed for the divalent ones: 14—15 water molecules existed in the range of 4.7 to 6.0 Å, a part of them presumably in the hollows along the C_2 axes of the complex, and only a single broad peak was observed around 7.7 Å as the hydrophobic hydration shell. These results indicated that the hydrophobic hydration structure was reduced by the increase of the ionic charge, as predicted from a comparison of temperature coefficients of the Walden product obtained by the conductivity measurements of dilute solutions.

Various hydrophobic interactions have been reported for tris(1,10-phenanthroline)metal or tris(2,2′-bipyridine)metal complexes in aqueous solutions,[1—8] mostly related to the hydrophobic association or aggregation which is caused by the free energy decrease based on the reduction of the hydrophobic hydration. Structural aspects of the hydrophobic hydration of these complex ions are not yet well-defined, although the water structure in their vicinity is presumed to be enhanced in view of the results of the conductivity measurements: the $[Fe(phen)_3]^{2+}$, $[Co(phen)_3]^{3+}$, and $[Co(bpy)_3]^{3+}$ ions could be classified as hydrophobic structure-makers, since the temperature coefficients of the Walden product of these complex ions had positive values similar to those of tetraalkylammonium ions.[9]

Many works on the hydration structure have been carried out for simple ions, using X-ray diffraction, neutron diffraction, and so on,[10] but few results exist for metal complex ions. This is mainly because the radial distribution function obtained from the diffraction measurements includes all structural information of various intra- and intermolecular interactions in solution, which make it difficult to extract the part of the hydration. Isomorphous substitution technique on the X-ray diffraction seems to be useful for the investigation of the hydration structure of metal complex ions, since this technique can give a radial distribution function having an origin at the metal center, giving only the interactions with the metal atom. Such an isomorphous substitution method, applicable to isostructural solutions containing metal ions or metal complex ions with different scattering powers, has been applied to the systems of erbium(III) and yttrium(III) ions in water[11,12] and in dimethyl sulfoxide,[13] cobalt(II) and magnesium(II) ions in *N*,*N*-dimethylformamide,[14] 5,10,15,20-tetra(4-sulfophenyl)porphinatopalladium(II) and copper(II) complex ions in water,[15] and tris(acetylacetonato)ruthenium(III) and chromium(III) complexes in acetonitrile.[16]

The present study was made in order to clarify the hydrophobic hydration structures around tris(1,10-phenanthro-

line)metal and tris(2,2′-bipyridine)metal complex ions by means of the X-ray diffraction method with the isomorphous substitution. The measurements were carried out for aqueous solutions of sulfates of $[Ru(phen)_3]^{2+}$, $[Ni(phen)_3]^{2+}$, $[Ru(bpy)_3]^{2+}$, $[Ni(bpy)_3]^{2+}$, $[Rh(bpy)_3]^{3+}$, and $[Cr(bpy)_3]^{3+}$ and chlorides of $[Ru(phen)_3]^{2+}$, $[Ni(phen)_3]^{2+}$, $[Rh(bpy)_3]^{3+}$, and $[Cr(bpy)_3]^{3+}$. The isomorphous substitution procedure was performed between ruthenium(II) and nickel(II) complexes or between rhodium(III) and chromium(III) complexes. Densities and conductivities of the dilute solutions were also measured to estimate the effective ionic radius, the closest distance of approach of ions, and the temperature coefficient of the Walden product. These results can give some important information about the ion–ion–solvent interactions.

Experimental and Theoretical

Materials. Chloride and sulfate of $[Ru(phen)_3]^{2+}$ were prepared in the manner described previously.[17,18] Chloride and sulfate of $[Ni(phen)_3]^{2+}$ were prepared from nickel chloride and nickel sulfate, respectively, in a manner similar to that described in the literature.[10] Preparations of sulfates of $[Ru(bpy)_3]^{2+}$ and $[Ni(bpy)_3]^{2+}$ were modeled on those of $[Ru(phen)_3]^{2+}$ and $[Ni(phen)_3]^{2+}$, respectively. These ruthenium(II) and nickel(II) complex salts were recrystallized from water by the addition of acetone. The chloride of $[Rh(bpy)_3]^{3+}$ was prepared according to the manner given in the literature.[20] The sulfate of $[Rh(bpy)_3]^{3+}$ was prepared by the double decomposition of the chloride of the complex with silver sulfate. Salts of $[Cr(bpy)_3]^{3+}$ were obtained by the oxidation of $[Cr(bpy)_3]Br_2$. The $[Cr(bpy)_3]^{2+}$ complex was prepared as bromide through the reaction of 2,2′-bipyridine with chromium(II) under the presence of ammonium bromide in a water–ethanol mixture by a modification of a procedure of the preparation of $[Cr(NH_3)_6]Cl_3$.[21] The chloride and sulfate of $[Cr(bpy)_3]^{3+}$ were obtained by the double decomposition using silver chloride and silver sulfate, respectively. These rhodium(III) and chromium(III) complex salts were recrystallized from water by the addition of ethanol and acetone. All salts were air-dried and identified by the visible-ultraviolet spectrum measurements. The number of water of crystallization ($n(H_2O)$) of the salts was determined by the Karl–Fischer method with an AQ-5 Aquacounter of Hiranuma Sangyo Co. The values of $n(H_2O)$ were 7.84 ($[Ru(phen)_3]Cl_2$), 7.02 ($[Ni(phen)_3]Cl_2$), 9.75 ($[Ru(phen)_3]SO_4$), 9.65 ($[Ni(phen)_3]SO_4$), 7.18 ($[Ru(bpy)_3]SO_4$), 7.16 ($[Ni(bpy)_3]SO_4$), 4.76 ($[Rh(bpy)_3]Cl_3$), 4.78 ($[Cr(bpy)_3]Cl_3$), 15.38 ($[Rh(bpy)_3]_2(SO_4)_3$), and 16.88 ($[Cr(bpy)_3]_2(SO_4)_3$). All chemicals used for the syntheses were of reagent grade; ruthenium(III) chloride and rhodium(III) chloride were purchased from Soekawa Chemical Co. and the other chemicals were purchased from Wako Pure Chemical Industries.

X-Ray Diffraction. Each pair of solutions used for the isomorphous substitution treatment was prepared by weight to give the same molar ratios of complex/water. Their molar concentrations were determined by measuring densities with a DA-310 Density/Specific Gravity Meter of Kyoto Electronics Co. Concentrations (c), densities (d), and absorption coefficients (μ) of solutions and stoichiometric unit volumes (V) containing one metal ion are given in Table 1.

The X-ray diffraction measurements were made with a Rigaku θ–θ diffractometer using Mo $K\alpha$ radiation ($\lambda = 0.7107$ Å) and a focusing LiF single-crystal monochromator at 26±1 °C in a manner similar to that described previously.[11,14,16] Intensities were collected at about four hundred points of 2θ between 1.6° and 140°. For each point, about 3×10^5 counts were accumulated. The change of the effective scattering angle from the geometrical one due to the low absorption of solution was corrected by estimating the position which gave a half of the observed scattering intensity. After the absorption correction the diffraction intensity data were treated by a version of the KURVLR program modified for use on an IBM personal computer.

Radial distribution functions were derived according to the manner previously described.[11,14,16] The radical distribution function, $D(r)$, involving all pair interactions (on the X-ray diffraction) in solution was obtained by

$$D(r) = 4\pi r^2\rho_0 + \frac{2r}{\pi}\int_0^{s_{max}} si(s)H(s)\sin(rs)\mathrm{d}s, \quad (1)$$

where $\rho_0=(\sum n_i Z_i)^2/V$, $s=4\pi\sin\theta/\lambda$, $i(s)$ is the reduced intensity per stoichiometric unit volume (V), and $H(s)$ is the modification

Table 1. Concentrations (c), Densities (d), Stoichiometric Unit Volumes (V), Absorption Coefficients (μ), and Electron Densities ($\rho_0{}^M$) of Solutions at 25 °C

System	Solution	Complex salt	c/mol dm^{-3}			d	V	μ	$\rho_0{}^M$
			Complex ion	Anion	H_2O	g cm^{-3}	Å^3	cm^{-1}	e^{2}Å^{-3}
RNPSO(A)	RUPSO(A)	$[Ru(phen)_3]SO_4$	0.7954	0.7954	36.24	1.240	2088	2.96	32.9
	NIPSO(A)	$[Ni(phen)_3]SO_4$	0.7929	0.7929	36.13	1.202	2094	3.44	
RNPSO(B)	RUPSO(B)	$[Ru(phen)_3]SO_4$	0.2553	0.2553	49.25	1.076	6505	1.67	29.9
	NIPSO(B)	$[Ni(phen)_3]SO_4$	0.2554	0.2554	49.17	1.064	6502	1.82	
RNPCL	RUPCL	$[Ru(phen)_3]Cl_2$	0.2105	0.4210	50.06	1.052	7889	1.65	29.3
	NIPCL	$[Ni(phen)_3]Cl_2$	0.2105	0.4210	50.04	1.043	7889	1.78	
RNBSO	RUBSO	$[Ru(bpy)_3]SO_4$	0.3972	0.3972	46.67	1.105	4181	2.01	30.4
	NIBSO	$[Ni(bpy)_3]SO_4$	0.3965	0.3965	46.59	1.086	4188	2.25	
RCBSO	RHBSO	$[Rh(bpy)_3]_2(SO_4)_3$	0.4957	0.7436	44.76	1.161	3350	2.45	32.5
	CRBSO	$[Cr(bpy)_3]_2(SO_4)_3$	0.4953	0.7429	44.71	1.135	3353	2.02	
RCBCL	RHBCL	$[Rh(bpy)_3]Cl_3$	0.7285	2.186	38.66	1.190	2280	3.56	32.6
	CRBCL	$[Cr(bpy)_3]Cl_3$	0.7282	2.185	38.64	1.153	2280	2.94	
	H_2O	(Pure water)			55.34	0.997	30.0	1.06	

function with the scattering factor of oxygen (f_O) and a damping factor k=0.01 Å^{-2}, that is, $H(s)=(f_O(0)/f_O(s))^2\exp(-ks^2)$. n_i is the number of atoms i with atomic number Z_i in V and the other symbols have their usual meanings. Spurious peaks below about 1 Å in $D(r)$ were removed to correct $i(s)$ for low-frequency additions. The radial distribution function, $D^M(r)$, including only metal interactions such as M–N or M–C was obtained by

$$D^M(r) = 4\pi r^2\rho_0^M + \frac{2r}{\pi}\int_0^{s_{max}} s\Delta i(s)F(s)H(s)\sin(rs)ds, \quad (2)$$

with

$$F(s) = \frac{f_M(s)}{f_M(s)—f_{M'}(s)}, \quad (3)$$

where $F(s)$ is the deconvolution factor, $\Delta i(s)$ is the difference in $i(s)$ between two isostructural solutions, and ρ_0^M indicates the terms concerning the metal M in ρ_0. The values of ρ_0^M are given in Table 1. The metal M corresponds to ruthenium(II) or rhodium(III) and the metal M′ corresponds to nickel(II) or chromium(III) in the present study.

The theoretical intensity, $i_{M-q}(s)$, for the interaction between the atoms M and q was given by

$$i_{M-q}(s) = 2n_q f_M(s)f_q(s)\frac{\sin\{r(M-q)\cdot s\}}{r(M-q)\cdot s}\exp\left(-\frac{l^2s^2}{2}\right), \quad (4)$$

where n_q is the number of atoms q in V and l is the root mean square variation of the distance r(M–q) related to the temperature factor(b) by $b=l^2/2$. The corresponding contribution, $P_{M-q}(r)$, to $D(r)$ is given by

$$P_{M-q}(r) = \frac{2r}{\pi}\int_0^{s_{max}} si_{M-q}(s)H(s)\sin(rs)ds. \quad (5)$$

The analysis of $D^M(r)$ was made by use of the following equation instead of Eq. 5, since a small difference was found between r(Ru–N) and r(Ni–N) or between r(Rh–N) and r(Cr–N) as described later.

$$P'_{M-q}(r) = \frac{2r}{\pi}\int_0^{s_{max}} s\{i_{M-q}(s) - i_{M'-q}(s)\}F(s)H(s)\sin(rs)ds. \quad (6)$$

The values of l and n_q in Eq. 4 were assumed to be the same between M–q and M′–q, respectively.

Conductivity. Conductivity measurements of aqueous solutions of $[Ru(phen)_3]SO_4$, $[Ni(phen)_3]SO_4$, and $[Ru(bpy)_3]SO_4$ were made by use of a Fuso 360 linear bridge conductometer at temperatures of 5 °C-intervals from 0 to 50 °C. Concentration of solutions was below 0.001 mol dm^{-3}. Further details of the experimental procedure have already been described.[9,22,33] The molar conductivities observed were analyzed by use of the Fuoss–Justice equation.[22] The limiting molar conductivities of the complex ions, λ^∞, were estimated from the analysis, using those of the sulfate ion given previously.[24]

Partial Molar Volume. Densities (25.0 °C) of aqueous solutions of sulfate or chloride of the complexes were measured at concentrations below 0.002 mol dm^{-3}, using a vibrating-tube SS-D-200 densimeter of Shibayama Scientific Co. Partial molar volumes of the salt at infinite dilution were obtained from the density data in the manner described previously[25] to estimate those of the complex ion by taking $V^\infty(SO_4^{2-})$=24.8 cm^3 mol^{-1} and $V^\infty(Cl^-)$=23.2 cm^3 mol^{-1}.[25]

Results and Discussion

Ion–Ion and Ion–Solvent Interactions and Effective Size of the Complex Ions in Dilute Aqueous Solutions.

Partial molar volumes of the complex ion at infinite dilution, V^∞(ion), obtained by the density measurements are shown in Table 2, together with the effective ionic radii, r_{ef}, estimated from V^∞(ion) by use of Glueckauf's equation.[25] The values of V^∞(ion) are found to be similar to each other between ruthenium and nickel complexes with the same ligands or between rhodium and chromium complexes, suggesting that the complex ions are almost isostructural. The large difference of V^∞(ion) between $[M(bpy)_3]^{2+}$ (M=Ru or Ni) and $[M(bpy)_3]^{3+}$ (M=Rh or Cr) is attributable to the difference of electrostriction power dependent on their ionic charge. The effective ionic radius (r_{ef}) corresponds to van der Waals one of the complex ion regarded as a sphere. The values of r_{ef} obtained for $[M(bpy)_3]^{2+}$ and $[M(bpy)_3]^{3+}$ are similar to each other, indicating the reasonableness of the use of Glueckauf's equation.

Molar conductivities of sulfate of divalent metal complexes observed were analyzed by use of the Fuoss–Justice equation,[22] considering the ion association between complex ion and sulfate ion on the assumption of the closest distance of approach of ions, a. Assuming the value of a around 7.3 Å equal to the sum of effective ionic radii ($\sum r_{ef}$) could not give an appreciable ion-association constant, contrary to the prediction from the ion-association theory,[26] suggesting that the actual closest distance is large, due to strong hydration of the ions and that no specific interaction is present between the ions. The best value of a was regarded as that giving an ion-association constant at infinite dilution, K_A, consistent with theoretical one.[26] The values of a and K_A at 25 °C obtained are summarized in Table 3, together with those of standard enthalpy change, $\Delta H°$, and standard entropy change, $\Delta S°$. That the closest distance of approach is larger than 11 Å implies that no contact ion pair is formed. Although the conductivity measurements were not made for the trivalent complex ions used in the present study, the information about the ion-association constant between $[Co(bpy)_3]^{3+}$ and Cl^- is available: K_A=31±2 dm^3 mol^{-1} at 25 °C with an assumption of a=6.6 Å equal to $\sum r_{ef}$,[9] slightly larger than a theoretical value of 23 dm^3 mol^{-1} with the same a value.[26] An assumption of a=5.6 Å gives K_A=28±2 dm^3 mol^{-1} consistent with a theoretical prediction.[26] These

Table 2. Partial Molar Volume (V^∞(ion)) and Effective Ionic Radius (r_{ef}) of the Complex Ions at 25 °C

Complex ion	V^∞(ion) / cm^3 mol^{-1}	r_{ef} / Å
$[Ru(phen)_3]^{2+}$	403±1	4.97
$[Ni(phen)_3]^{2+}$	405±1	4.98
$[Ru(bpy)_3]^{2+}$	366±2	4.80
$[Ni(bpy)_3]^{2+}$	369±2	4.82
$[Rh(bpy)_3]^{3+}$	338±2	4.80
$[Cr(bpy)_3]^{3+}$	340±2	4.81
$[Co(bpy)_3]^{3+}$	333±2[a]	4.78[a]
$[Co(phen)_3]^{3+}$	374±2[a]	4.96[a]

a) Ref. 9.

Table 3. Thermodynamic Parameters of the Ion Association at 25 °C: Closest Distance of Approach of Ions (a), Ion-Association Constant (K_A), Standard Enthalpy Change ($\Delta H°$), and Standard Entropy Change ($\Delta S°$) at Infinite Dilution

Complex salt	a	K_A	$\Delta H°$	$\Delta S°$
	Å	$dm^3\ mol^{-1}$	$kJ\ mol^{-1}$	$J\ K^{-1}\ mol^{-1}$
$[Ru(phen)_3]SO_4$	12.0	38±3	3.9±0.2	43.3±0.5
$[Ni(phen)_3]SO_4$	11.7	39±2	3.3±0.2	41.4±0.4
$[Ru(bpy)_3]SO_4$	11.1	41±2	3.5±0.2	42.6±0.5

results suggest that the chloride ion can form a contact ion pair with the trivalent complex ion. The values of a and K_A between $[M(bpy)_3]^{3+}$ and SO_4^{2-} may be comparable to 8.9 Å and 324±10 $dm^3\ mol^{-1}$, respectively, obtained for the $[Co(phen)_3]^{3+}$ and SO_4^{2-} ions.[27]

The limiting molar conductivity, $\lambda^\infty(M^{2+}/2, t)$, of the divalent complex ion obtained could be given as a function of temperature (t in °C) by the equation:

$$\lambda^\infty(M^{2+}/2,t)=\lambda^\infty(1/2,25\ °C)+\alpha(t-25)+\beta(t-25)^2+\gamma(t-25)^3, \quad (7)$$

where M^{2+} expresses the divalent complex ion and $\lambda^\infty(M^{2+}/2, t)$ corresponds to the limiting molar conductivity per 1/2 mol dm^{-3}. Values of the parameters in Eq. 7, summarized in Table 4, are close to each other between the $[Ru(phen)_3]^{2+}$ and $[Ni(phen)_3]^{2+}$ ions. Stokes radii, r_s, at 25 °C and ratios of r_s to r_{ef} are shown in Table 5. The size of the $[Ni(phen)_3]^{2+}$ ion seems to be slightly larger than the $[Ru(phen)_3]^{2+}$ ion from a comparison of r_s or r_{ef} values. Temperature coefficients of the Walden product, $d\ln(\lambda^\infty\eta_0)/dT$, at 25 °C ($\eta_0$ is the viscosity coefficient of pure water), given in Table 5, have positive values, similarly to those of tetraalkylammonium ions, indicating that the complex ions can be classified as hydrophobic structure-makers.[9,28] Values of r_s/r_{ef} larger than unity suggest that the fluidity of solvent is decreased in the vicinity of the complex ions. Such a decrease in fluidity of solvent has been indicated by the viscosity measurements of aqueous solutions of some complex salts: the B(ion) coefficients of the Jones–Dole equation for $[Co(phen)_3]^{2+}$, $[Co(phen)_3]^{3+}$, $[Co(bpy)_3]^{2+}$, and $[Co(bpy)_3]^{3+}$ were reported to be 1.61, 1.53, 1.37, and 1.31 $dm^3\ mol^{-1}$, respectively.[29] Large positive values of the B(ion) coefficient, revealing the decrease in fluidity of solvent, suggest the presence of hydrophobic hydration structure, although the contribution based on the following Einstein term (B_E) should be subtracted from B(ion):

Table 5. Stokes Radius (r_s), Ratio of r_s to r_{ef}, and Temperature Coefficient of Walden Product ($d\ln(\lambda^\infty\eta_0)/dT$) at 25 °C

Complex ion	r_s	r_s/r_{ef}	$d\ln(\lambda^\infty\eta_0)/dT$
	Å		K^{-1}
$[Ru(phen)_3]^{2+}$	5.18	1.04	0.0018±0.0001
$[Ni(phen)_3]^{2+}$	5.24	1.05	0.0020±0.0001
$[Ru(bpy)_3]^{2+}$	4.99	1.04	0.0021±0.0001
$[Co(bpy)_3]^{3+}$	4.90[a]	1.03[a]	0.0011±0.0001[a]
$[Co(phen)_3]^{3+}$	5.13[a]	1.03[a]	0.0012±0.0001[a]

a) Ref. 9.

$B_E=2.5V_{ion}$ where V_{ion} is approximated as $4\pi r_{ef}^3 N_A/3$, an assumption of $r_{ef}=4.8$ Å gives $B_E=0.70$ $dm^3\ mol^{-1}$ smaller than the values of B(ion). The positive temperature coefficient of the Walden product implies that the decrease of fluidity diminishes with increasing temperature because of destruction of the hydrophobic hydration structure. From a comparison of the $d\ln(\lambda^\infty\eta_0)/dT$ values given in Table 5, we think that the divalent complex ions are probably more hydrophobic than the trivalent ones, although this is not necessarily obvious from the values of r_s, r_s/r_{ef}, and B(ion). Such a charge dependence suggests that hydrophobic properties of the complex ions are weakened with increasing their ionic charge, as pointed out in the previous paper.[9]

Structure of the Complex Ions in Solutions Observed by the X-Ray Diffraction Method. Radial distribution functions, $D(r)$, obtained by use of Eq. 1 for the 0.80 M (M=mol dm^{-3}) solutions of $[Ru(phen)_3]SO_4$ (RUPSO(A)) and $[Ni(phen)_3]SO_4$ (NIPSO(A)) are shown in Fig. 1a, compared with that of pure water scaled to give the same number of water molecules as in the solutions. Corresponding differential radial distribution functions, $D(r)-4\pi r^2\rho_0$, expressing the deviation from the average electron density distribution, are given in Fig. 2, together with those of some other solutions. The $D(r)$ curves include all interactions in solutions: intramolecular interactions of H_2O, phen, and SO_4^{2-} and intermolecular interactions of H_2O–H_2O, H_2O–phen, H_2O–SO_4^{2-}, phen–phen, phen–SO_4^{2-}, and SO_4^{2-}–SO_4^{2-}, in addition to metal interactions (M–phen, M–H_2O, M–SO_4^{2-}, and M–M). The metal interactions are located at positions which exhibit some difference between two solutions in Fig. 1a. Figure 1b shows the residual curves of $D(r)$ obtained by removing intramolecular interactions of H_2O and intermolecular H_2O–H_2O interactions approximated by the $D(r)$ function of pure water, and by removing the intramolecular interactions of SO_4^{2-} and of the phen

Table 4. Parameter Values of Eq. 7

Complex ion	λ^∞ ($M^{2+}/2$, 25 °C)	α	$\beta\times10^3$	$\gamma\times10^5$
	$S\ cm^2\ mol^{-1}$	$S\ cm^2\ mol^{-1}\ K^{-1}$	$S\ cm^2\ mol^{-1}\ K^{-2}$	$S\ cm^2\ mol^{-1}\ K^{-3}$
$[Ru(phen)_3]^{2+}$	35.56	0.873	4.36	−3.0
$[Ni(phen)_3]^{2+}$	35.16	0.872	4.49	−3.0
$[Ru(bpy)_3]^{2+}$	36.94	0.919	4.79	−3.4

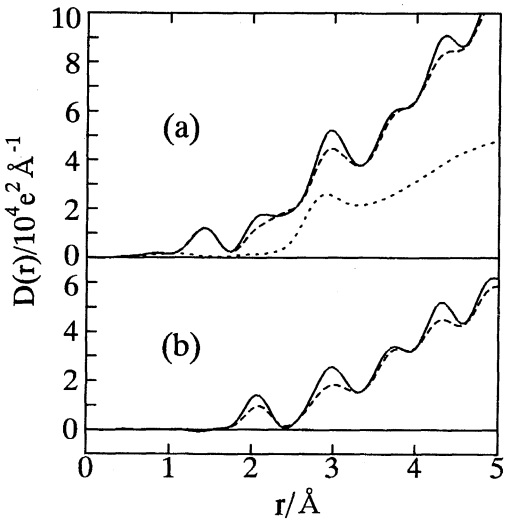

Fig. 1. (a) Radial distribution functions, $D(r)$, for the 0.8 M solutions of $[Ru(phen)_3]SO_4$ (RUPSO(A), solid line) and $[Ni(phen)_3]SO_4$ (NIPSO(A), dashed line) and $D(r)$ for pure water (dotted line). (b) Residual curves of $D(r)$ for the corresponding solutions, obtained by eliminating intra- and intermolecular interactions of H_2O, intramolecular interactions of SO_4^{2-}, and those of the phen ligand within 2.4 Å.

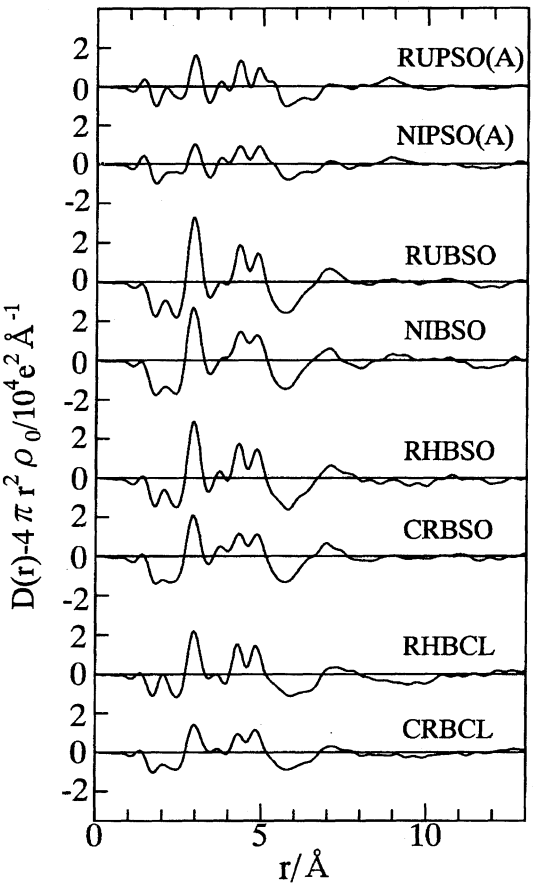

Fig. 2. Differential radial distribution functions, $D(r) - 4\pi r^2\rho_0$, for the solutions of $[Ru(phen)_3]SO_4$ (RUPSO(A): 0.80 M), $[Ni(phen)_3]SO_4$ (NIPSO(A): 0.80 M), $[Ru(bpy)_3]SO_4$ (RUBSO), $[Ni(bpy)_3]SO_4$ (NIBSO), $[Rh(bpy)_3]_2(SO_4)_3$ (RHBSO), $[Cr(bpy)_3]_2(SO_4)_3$ (CRBSO), $[Rh(bpy)_3]Cl_3$ (RHBCL), and $[Cr(bpy)_3]Cl_3$ (CRBCL).

ligand within 2.4 Å, which were regarded as r(S–O)=1.47 Å (l=0.04 Å), r(O–O)=2.40 Å (l=0.08 Å), r(C–C)=1.38 Å (l=0.04 Å) and 2.39 Å (l=0.06 Å), and r(C–N)=1.38 Å (l=0.04 Å) and 2.39 Å (l=0.06 Å). The first peaks in residual $D(r)$ functions, located at 2.05 and 2.07 Å, correspond to the Ru–N and Ni–N interactions, respectively, indicating that the isomorphous substitution treatment is effective between ruthenium and nickel complexes although they are not completely isostructural. This incompleteness was considered on the analysis of radial distribution functions in the following discussion.

Figure 3 shows the radial distribution function, $D^{Ru}(r)$, obtained by the isomorphous substitution between the 0.80 M solutions of $[Ru(phen)_3]SO_4$ (RUPSO(A)) and $[Ni(phen)_3]SO_4$ (NIPSO(A)), using Eq. 2 with M=Ru. The axis of abscissa, r, corresponds to the distance from the metal atom. Six peaks are found in the range of $r<6$ Å and the five peaks except a small peak around 3.5—3.6 Å (the third peak) are attributable to the intramolecular metal interactions within the complex ions; the third peak will be discussed later. The first peak corresponding to nitrogen atoms bonded to the metal atom, located apparently at r=2.03 Å, was analyzed by regarding the bond length difference, r(Ni–N)$-r$(Ru–N), as 0.02 Å. The values of r(Ru–N) and r(Ni–N) were determined to be 2.05 and 2.07 Å, respectively, and the number of nitrogen atoms was n=6.0(2). The second peak around 2.9 Å corresponds to carbon atoms: C_2, C_9, C_{10a}, and C_{10b} (group C_A), of the phen ligand shown in Fig. 4. The fourth peak around 4.3 Å can be assigned to the C_3, C_8, C_{4a}, and C_{6a} atoms (group C_B). The fifth peak around 4.8 Å reflects the C_4 and C_7 atoms (group C_C) and the sixth peak around 5.3 Å includes the C_5 and C_6 atoms (group C_D).

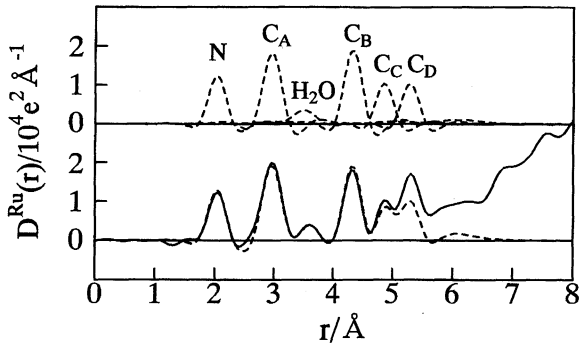

Fig. 3. Radial distribution function, $D^{Ru}(r)$, for the 0.80 M solutions of $[M(phen)_3]SO_4$ (RNPSO(A), solid line), the theoretical curves of metal–phen and metal–H_2O interactions (upper dashed lines), and the sum of the theoretical curves (lower dashed line).

These peaks were theoretically analyzed by taking the numbers of carbon atoms as formal ones within the complex ion, and by assuming r(Ni–C_i)$-r$(Ru–C_i)=0.02 Å, where C_i corresponds to C_A, C_B, C_C, or C_D, for the following reason.

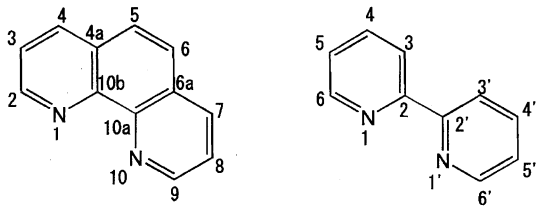

Fig. 4. Structure formulae of 1,10-phenanthroline (phen) and 2,2′-bipyridine (bpy).

The difference, r(Ni–N) − r(Ru–N)=0.02 Å, means that the distance from the nickel atom to the ligand molecule center along the C_2 axis is extended by about 0.027 Å than that for the ruthenium atom from the geometrical consideration. Then, the value of r(Ni–C) − r(Ru–C) for each carbon atom is somewhat larger than 0.02 Å for C_5, C_6, C_{4a}, C_{6a}, C_{10a}, or C_{10b}, somewhat smaller than 0.02 Å for C_2, C_3, C_8, or C_9, and close to 0.02 Å for C_4 or C_7 (group C_C). The r(Ni–C_i) − r(Ru–C_i) corresponds to the average of r(Ni–C) − r(Ru–C) in each carbon group, of which value becomes close to 0.02 Å for C_A or C_B.

The structure parameters obtained are summarized in Table 6, where the values of r(Ni–N) and r(Ni–C_i) not given are longer by 0.02 Å than those of r(Ru–N) and r(Ru–C_i), respectively. Theoretical curves with these structure parameters are depicted in Fig. 3, considering also Ru–H_i interactions about hydrogen atoms of the phen ligand: The values of r(Ru–H_i) were taken as 3.1 Å (H_A=H_2, H_9), 5.1 Å (H_B=H_3, H_8), 5.9 Å (H_C=H_4, H_7), and 6.3 Å (H_D=H_5, H_6) by taking into account Ru–C_i distances obtained, the framework of the phen ligand (Fig. 4), and positions of hydrogen atoms in the crystal of $[Ru(phen)_3]Br_2 \cdot 6.5H_2O$.[30] The values of l were regarded as 0.14 Å.

The $D^{Ru}(r)$ functions obtained for the solutions of 0.26 M $[M(phen)_3]SO_4$ (RNPSO(B)) and 0.21 M $[M(phen)_3]Cl_2$ (RNPCL) are shown in Fig. 5. Irregularity and distortion in $D^{Ru}(r)$ for these solutions are larger than those for the 0.80 M solutions of $[M(phen)_3]SO_4$ (RNPSO(A)), and some spurious peaks appear over about 6 Å, due to low concentrations giving smaller $\Delta i(s)/i(s)$ values, but metal–ligand atom distance were only a little changed, as shown in Table 6. The

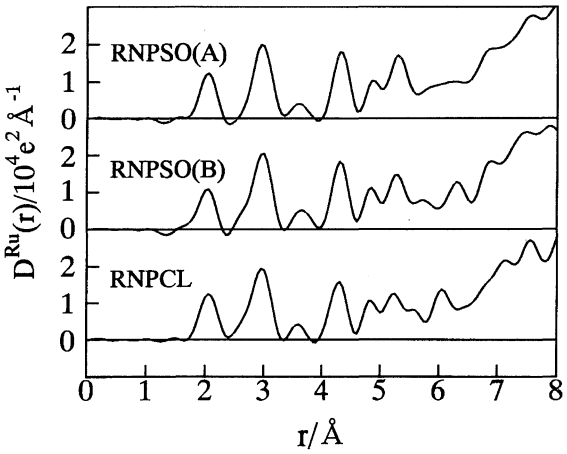

Fig. 5. Radial distribution functions, $D^{Ru}(r)$, for the solutions of $[M(phen)_3]SO_4$ (RNPSO(A): 0.80 M, RNPSO(B): 0.26 M) and $[M(phen)_3]Cl_2$ (RNPCL).

Ru–N and Ru–C_i distances in the solutions were essentially consistent with those in the crystal[30] given in Table 6. The Ni–N and Ni–C_i distances obtained were also comparable to those in the crystal of $K[Ni(phen)_3][Co(C_2O_4)_3] \cdot 2H_2O$:[31] 2.10 Å(N), 2.98 Å($C_A$), 4.38 Å($C_B$), 4.88 Å($C_C$), and 5.33 Å($C_D$), where the value of r(Ni–N) is an average of two kinds of different bond lengths, 2.06(3) and 2.15(3) Å, indicating the presence of some distortion due to the surroundings or the crystal packing.

The Ru–N distance in $[Ru(bpy)_3]^{2+}$ and the Ni–N distance in $[Ni(bpy)_3]^{2+}$, estimated from the analyses of $D(r)$ functions of their sulfate solutions, were the same as those in $[Ru(phen)_3]^{2+}$ and $[Ni(phen)_3]^{2+}$, respectively. The $D^{Ru}(r)$ function obtained by the isomorphous substitution is shown in Fig. 6. Four distinct peaks in the range of r<5 Å, except a small peak around 3.5—3.6 Å, could be assigned to intramolecular metal interactions and were analyzed by taking r(Ni–N) − r(Ru–N)=r(Ni–C_i) − r(Ru–C_i)=0.02 Å. The Ru–N and Ru–C_i distances obtained are summarized in Table 7. The corresponding theoretical curves are depicted in Fig. 6, taking r(Ru–H_i)=3.1 Å (H_A=H_6, $H_{6'}$), 5.1 Å (H_B=H_3, $H_{3'}$, H_5, $H_{5'}$), and 5.9 Å (H_C=H_4, $H_{4'}$) with l=0.14 Å. The Ru–N and Ru–C_i distances in the crystals of $[Ru(bpy)_3](PF_6)_2$[32] and $[Ru(bpy)_3]_2[Co(CN)_6]Cl \cdot 8H_2O$[33] are also shown in Table 7.

Table 6. Structure Parameters of Intramolecular Interactions within $[Ru(phen)_3]^{2+}$

		In the solution of 0.80 M sulfate		In the solution of 0.26 M sulfate	0.21 M chloride	In the crystal of bromide[a]
Interactions	n[b]	r/Å	l/Å	r/Å	r/Å	r/Å
Ru–N	6	2.05(1)	0.08(1)	2.05(1)	2.06(1)	2.049(9)
Ru–C_A (C_2,C_9,C_{10a},C_{10b})	12	2.98(1)	0.11(1)	2.99(1)	2.98(1)	2.98 { 2.883(14) (C_{10a},C_{10b}); 3.068(8) (C_2,C_9) }
Ru–C_B (C_3,C_8,C_{4a},C_{6a})	12	4.35(2)	0.10(1)	4.34(2)	4.32(2)	4.32 { 4.253(11) (C_{4a},C_{6a}); 4.380(17) (C_3,C_8) }
Ru–C_C (C_4,C_7)	6	4.88(2)	0.08(1)	4.85(2)	4.85(2)	4.849(18)
Ru–C_D (C_5,C_6)	6	5.31(3)	0.08(1)	5.29(3)	5.26(3)	5.264(15)

a) $[Ru(phen)_3]Br_2 \cdot 6.5H_2O$ (Ref. 30). b) Numbers of atoms were fixed.

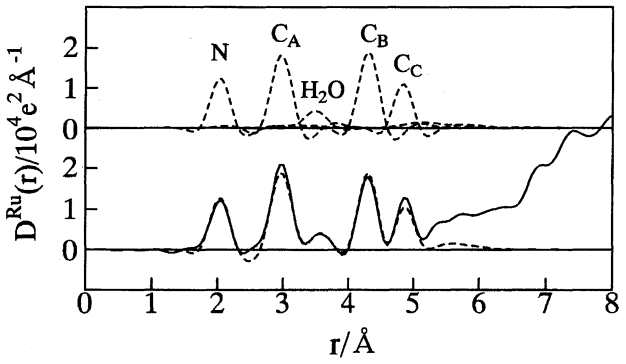

Fig. 6. Radial distribution function, $D^{Ru}(r)$, for the solutions of $[M(bpy)_3]SO_4$ (RNBSO, solid line), the theoretical curves of metal–bpy and metal–H_2O interactions (upper dashed lines), and the sum of the theoretical curves (lower dashed line).

Nitrogen and carbon atoms of the bpy ligand in the crystal of $[Ni(bpy)_3]SO_4 \cdot 7.5H_2O$[34] were located at 2.09 Å(N), 3.00 Å(C_A), 4.33 Å(C_B), and 4.87 Å(C_C) from the nickel atom.

The M–N distances in $[Rh(bpy)_3]^{3+}$ and $[Cr(bpy)_3]^{3+}$ were estimated to be r(Rh–N)=2.04 Å and r(Cr–N)=2.03 Å from the analyses of $D(r)$ functions of the sulfate solutions, and r(Rh–N)=2.03 Å and r(Cr–N)=2.04 Å from those of the chloride solutions. The $D^{Rh}(r)$ functions obtained from the solutions of sulfate and chloride of $[M(bpy)_3]^{3+}$ are shown in Figs. 7a and 7b, respectively. Four distinct peaks within 5 Å, assigned to intramolecular metal interactions, were analyzed by regarding r(Rh–N)$-r$(Cr–N) or r(Rh–C_i)$-r$(Cr–C_i) as 0.01 Å (sulfate) and −0.01 Å (chloride). The results are summarized in Table 8 and the corresponding theoretical curves are drawn in Fig. 7, taking r(Rh–H_i)=3.0 Å (H_A=H_6, $H_{6'}$), 5.0 Å (H_B=H_3, $H_{3'}$, H_5, $H_{5'}$), and 5.8 Å (H_C=H_4, $H_{4'}$) with l=0.14 Å. The Rh–N and Rh–C_i distances in the crystal of $[Rh(bpy)_3]Cl_3 \cdot 4H_2O$[35] are also given in Table 8. In the crystal of $[Cr(bpy)_3](PF_6)_3$[36] metal interaction distances were 2.04 Å (Cr–N), 2.97 Å (Cr–C_A), 4.26 Å (Cr–C_B), and 4.79 Å (Cr–C_C). The values of r(M–N) and r(M–C_i) in the solutions are in good agreement with those in the crystals.

Hydrophobic Hydrations Structure of $[M(phen)_3]^{2+}$ and $[M(bpy)_3]^{2+}$ (M=Ru and Ni). Similar peaks to that located around 3.5—3.6 Å of $D^{Ru}(r)$ in Fig. 3 for the 0.80 M solutions of $[M(phen)_3]SO_4$ (RNPSO(A)) are also found in Fig. 5 for the solutions of 0.26 M $[M(phen)_3]SO_4$ (RNPSO(B)) and 0.21 M $[M(phen)_3]Cl_2$ (RNPCL) as well as in Fig. 6 for the solutions of $[M(bpy)_3]SO_4$ (RNBSO). These peaks could not be attributed to any intramolecular interaction within the complex ion, but seemed to reflect some real atoms, even if background ripples might be overlapping more or less, considering their peak positions and intensities. We presumed that the peak around 3.5—3.6 Å could be ascribed to the closest water molecules for the complex ions. From the analyses of $D^{Ru}(r)$, the Ru–H_2O distance and the number of water molecules were estimated to be r=3.52(5) Å and n=1.8(3) in 0.80 M $[M(phen)_3]SO_4$, r=3.63(5) Å and n=2.0(3) in 0.26 M $[M(phen)_3]SO_4$, r=3.53(5) Å and n=1.4(3) in 0.21 M $[M(phen)_3]Cl_2$, and r=3.51(5) Å and n=1.8(3) in 0.40 M $[M(bpy)_3]SO_4$, respec-

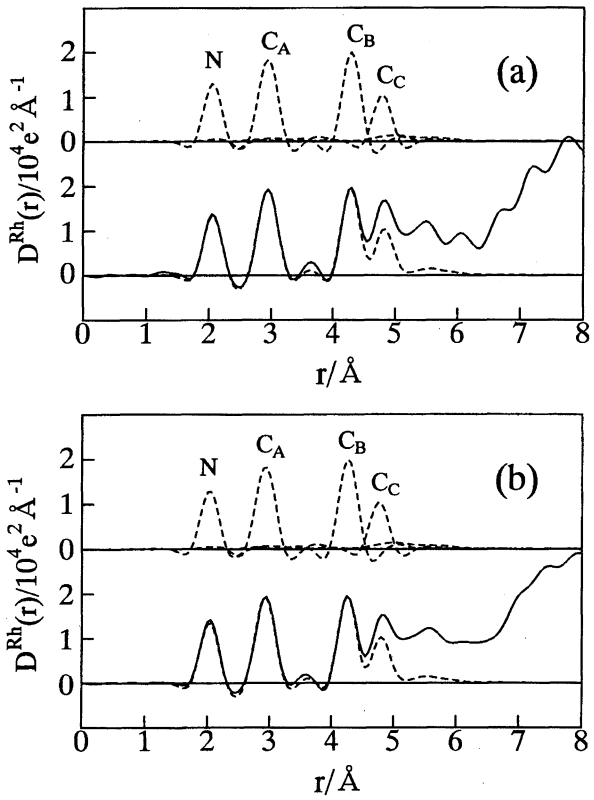

Fig. 7. Radial distribution functions, $D^{Rh}(r)$, for the solutions of $[M(bpy)_3]^{3+}$ (solid lines) and the theoretical curves of metal–bpy interactions (dashed lines). (a) $[M(bpy)_3]_2(SO_4)_3$ (RCBSO); (b) $[M(bpy)_3]Cl_3$ (RCBCL).

Table 7. Structure Parameters of Intramolecular Interactions within $[Ru(bpy)_3]^{2+}$

Interactions	In the solution			In the crystal[a)]	In the crystal[b)]
	n[c)]	r/Å	l/Å	r/Å	r/Å
Ru–N	6	2.05(1)	0.08(1)	2.05_6	2.067(16)
Ru–C_A (C_2,$C_{2'}$,C_6,$C_{6'}$)	12	2.99(1)	0.11(1)	2.99 { 2.92_4 (C_2,$C_{2'}$) 3.05_4 (C_6,$C_{6'}$) }	2.992 { 2.918(24) (C_2,$C_{2'}$) 3.065(10) (C_6,$C_{6'}$) }
Ru–C_B (C_3,$C_{3'}$,C_5,$C_{5'}$)	12	4.33(2)	0.10(1)	4.28 { 4.23_1 (C_3,$C_{3'}$) 4.33_4 (C_5,$C_{5'}$) }	4.303 { 4.253(18) (C_3,$C_{3'}$) 4.353(24) (C_5,$C_{5'}$) }
Ru–C_C (C_4,$C_{4'}$)	6	4.86(3)	0.07(1)	4.80_7	4.836(23)

a) $[Ru(bpy)_3](PF_6)_2$ (Ref. 32). b) $[Ru(bpy)_3]_2[Co(CN)_6]Cl \cdot 8H_2O$ (Ref. 33). c) Numbers of atoms were fixed.

Table 8. Structure Parameters of Intramolecular Interactions within $[Rh(bpy)_3]^{3+}$

		In the solution of sulfate		In the solution of chloride		In the crystal of chloride[a]
Interactions	n[b]	r/Å	l/Å	r/Å	l/Å	r/Å
Rh–N	6	2.04(1)	0.06(1)	2.03(1)	0.06(1)	2.036(3)
Rh–C_A (C_2,$C_{2'}$,C_6,$C_{6'}$)	12	2.93(1)	0.11(1)	2.93(1)	0.11(1)	2.95 { 2.873(16) (C_2,$C_{2'}$); 3.032(11) (C_6,$C_{6'}$) }
Rh–C_B (C_3,$C_{3'}$,C_5,$C_{5'}$)	12	4.28(2)	0.09(1)	4.27	0.09(1)	4.27 { 4.223(15) (C_3,$C_{3'}$); 4.322(7) (C_5,$C_{5'}$) }
Rh–C_C (C_4,$C_{4'}$)	6	4.78(3)	0.08(1)	4.77	0.08(1)	4.794(28)

a) $[Rh(bpy)_3]Cl_3 \cdot 4H_2O$ (Ref. 35). b) Numbers of atoms were fixed.

tively; their theoretical curves are drawn for the solutions of 0.80 M $[M(phen)_3]SO_4$ and 0.40 M $[M(bpy)_3]SO_4$ in Figs. 3 and 6, respectively. These results imply that about two water molecules exist in the range of 3.5 to 3.6 Å. Their most probable positions are in two peripheral hollows along the C_3 axis of the complex ions, probably containing one water molecule in one hollow, considering the shape of the hollows, the distance from the metal atom, the hollows along the C_2 axes being less hydrophilic in the crystals,[30,33,34] and the number of the closest water molecules being about two. However, no water molecule around 3.5—3.6 Å was found in the crystals: the closest water molecule was located at 5.05 Å in $[Ru(phen)_3]Br_2 \cdot 6.5H_2O$,[30] at 5.68 Å in $[Ru(bpy)_3]_2[Co(CN)_6]Cl \cdot 8H_2O$,[33] and at 5.47 Å in $[Ni(bpy)_3]SO_4 \cdot 7.5H_2O$.[34] This is because, in the crystals, the number of water molecules are not enough to permit the same hydration state as in the solution.

Considering the structure of the complex ions in the crystal, shown in Fig. 8, the water molecule is allowed to approach within 5.0 Å, but the approach to the distance of 3.5—3.6 Å needs some geometrical change of the complex ion. That is, each phen or bpy ligand molecule must be twisted a little around a C_2 axis piercing itself to make it easier for the water molecules to approach more closely along the C_3 axis, keeping the D_3 symmetry of the complex ion as well as Ru–N bond lengths. The energy required for such a geometrical change may be provided by the following anisotropic hydration force: the ion–solvent electrostatic attraction force along the C_3 axis is probably stronger than that in the direction perpendicular to the C_3 axis. In the crystals of $[Ru(phen)_3]Br_2 \cdot 6.5H_2O$[30] and $[Ni(bpy)_3]SO_4 \cdot 7.5H_2O$,[34] the situation in the latter direction containing the C_2 axes is quite different from that in the solution, that is, complex ions are surrounded by adjacent complex ions and form a hydrophobic layer, probably with some intermolecular attraction force; water molecules and anions form a hydrophilic planar layer, having hydrogen-bonded network structure, sandwiched by the hydrophobic layers.

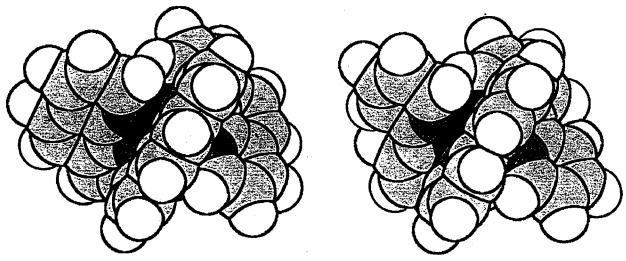

$[Ru(phen)_3]^{2+}$ $[Ru(bpy)_3]^{2+}$

Fig. 8. Structure of the $[Ru(phen)_3]^{2+}$ and $[Ru(bpy)_3]^{2+}$ complexes in the crystals of $[Ru(phen)_3]Br_2 \cdot 6.5H_2O$[30] and $[Ru(bpy)_3](PF_6)_2$,[32] respectively.

The theoretical peaks due to the metal–ligand interaction and the metal–water interaction around 3.5—3.6 Å were removed from $D^{Ru}(r)$ in order to make it easier to see the distribution of other molecules. Such $D^{Ru}(r)$ curves for the solutions of 0.80 M $[M(phen)_3]SO_4$ (RNPSO(A)) and 0.40 M $[M(bpy)_3]SO_4$ (RNBSO) are shown in Fig. 9. In each $D^{Ru}(r)$ curve, the practical distribution is found to start from about 5 Å and to continue up to about 6.5 Å, where a significant jump appears. The distribution in this region was attributed to water molecules, because no sulfate ion was presumed to

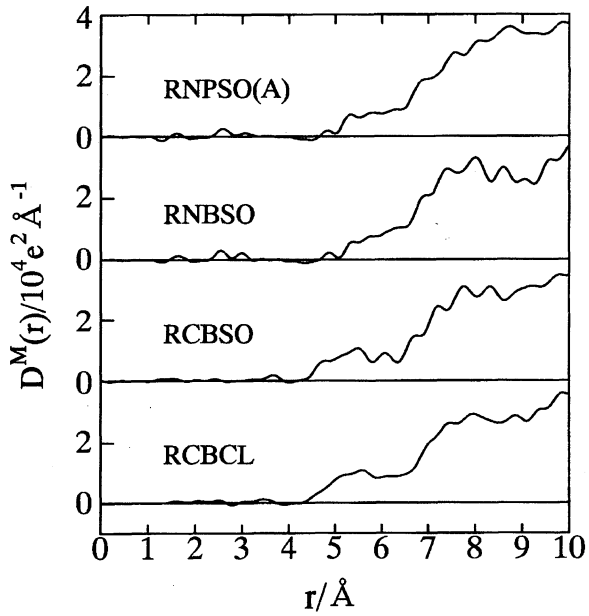

Fig. 9. Residual $D^{Ru}(r)$ and $D^{Rh}(r)$ curves obtained by eliminating the theoretical curves depicted in Figs. 3, 6, 7a, and 7b for the solutions of $[M(phen)_3]SO_4$ (RNPSO(A): 0.80 M), $[M(bpy)_3]SO_4$ (RNBSO), $[M(bpy)_3]_2(SO_4)_3$ (RCBSO), and $[M(bpy)_3]Cl_3$ (RCBCL).

be present, considering the results of conductivity measurements as well as the position of sulfate ion in the crystal of $[Ni(bpy)_3]SO_4 \cdot 7.5H_2O$,[34] where Ni–S and Ni–O distances of the closest sulfate ion were 8.28 and 7.56 Å, respectively. The first group of the water molecules in the solutions was located at $r(Ru–H_2O)=5.34(5)$ Å with $l=0.11$ Å and $n=3.0(5)$ in 0.80 M $[M(phen)_3]SO_4$, and at $r(Ru–H_2O)=5.44(5)$ Å with $l=0.11$ Å and $n=2.7(5)$ in 0.40 M $[M(bpy)_3]SO_4$. The distributions of subsequent water molecules were estimated as: $n(H_2O)=3.5$ around $r=5.8$ Å and $n(H_2O)=3.7$ around $r=6.2$ Å in 0.80 M $[M(phen)_3]SO_4$, $n(H_2O)=3.6$ around $r=5.9$ Å and $n(H_2O)=4.3$ around $r=6.3$ Å in 0.40 M $[M(bpy)_3]SO_4$; these values may involve some arbitrariness or uncertainties because no distinct peak is found in $D^{Ru}(r)$. The sums of water molecules in this region were 10.2 between 5.3 and 6.2 Å for $[M(phen)_3]^{2+}$ and 10.6 between 5.4 and 6.3 Å for $[M(bpy)_3]^{2+}$. These water molecules probably exist in the vicinity of two hollows along the C_3 axis of the complex ions. A large part of them may be in contact with the $H_2(H_8)$ and/or $H_3(H_9)$ atoms of phen ligand or with the $H_5(H_{5'})$ and/or $H_6(H_{6'})$ atoms of bpy ligand, and hydrogen-bonded to adjacent water molecules including the closest ones.

The jump of $D^{Ru}(r)$ around 6.5 Å in Fig. 9 is related to a large broad peak located in the region of 6.5 to 9.5 Å of the $D^{Ru}(r)-4\pi r^2\rho_0^{Ru}$ curves shown in Fig. 10. Similar broad peaks having high electron density are also recognized in the solutions of 0.26 M $[M(phen)_3]SO_4$ (RNPSO(B)) and 0.21 M $[M(phen)_3]Cl_2$ (RNPCL), as shown in Fig. 10, although they involve many narrow spurious peaks because of lower complex concentration. These broad peaks were attributed to the hydration shell surrounding the complex ions, because they were almost independent of concentrations of complex ion and counter ion as well as of kinds of counter ions, and because they could not be explained by the hydrophobic interaction between the complex ions observed by the NMR measurements.[6] The centers of the hydration shell were located around 8.0 and 7.7 Å from the central metal atoms of the $[M(phen)_3]^{2+}$ and $[M(bpy)_3]^{2+}$ ions, respectively, and the thickness of hydration shell of the $[M(bpy)_3]^{2+}$ ion was thinner than that of the $[M(phen)_3]^{2+}$ ion. Such a difference is due to a slightly smaller size and rounder shape of the $[M(bpy)_3]^{2+}$ ion compared with the $[M(phen)_3]^{2+}$ ion. The hydration shell observed can probably be classified into the hydrophobic hydration shell which is constituted by water molecules and anions, having the hydrogen-bonded network enhanced more than that in pure water. Distinct observation of the hydration shell suggests that the shell has a rather round shape and surrounds the complex ion while keeping the vacant spaces in peripheral hollows along the C_2 axes of the complex ion.

The distance of 7.7 Å from the metal atom of $[M(bpy)_3]^{2+}$ to the center of the hydration shell is equal to $r(Ru–H_B)$ plus 2.6 Å. This additional distance is close to the van der Waals contact distance between hydrogen atom of the bpy ligand and oxygen atom of water molecule. The intersection point between the $D^{Ru}(r)-4\pi r^2\rho_0^{Ru}$ curve of $[M(bpy)_3]^{2+}$ and the abscissa is located around 8.5 Å, close to the sum of $r(Ru–H_C)$

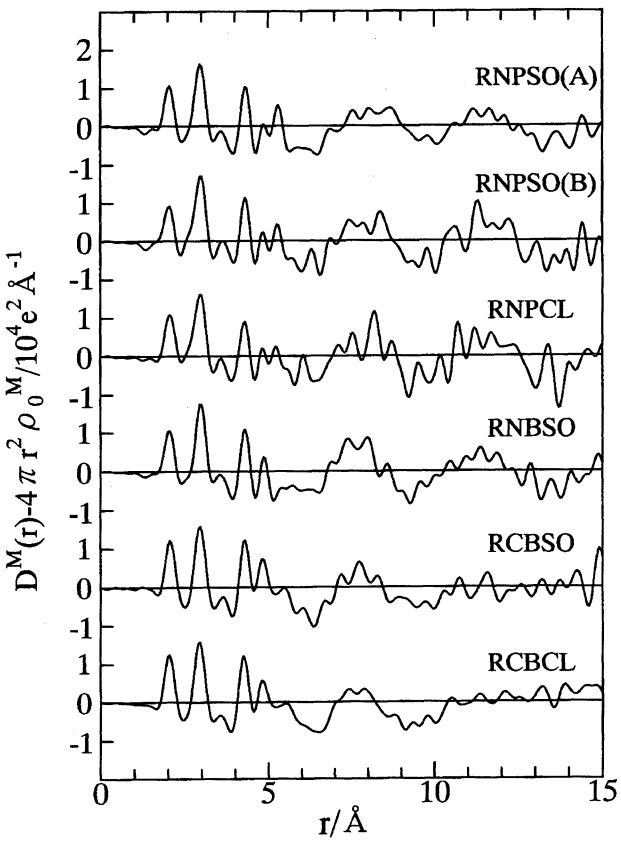

Fig. 10. Differential radial distribution functions, $D^{Ru}(r)-4\pi r^2\rho_0^{Ru}$ for the solutions of divalent complex salts: $[M(phen)_3]SO_4$ (RNPSO(A): 0.80 M), $[M(phen)_3]SO_4$ (RNPSO(B): 0.26 M), $[M(phen)_3]Cl_2$ (RNPCL), and $[M(bpy)_3]SO_4$ (RNBSO), and $D^{Rh}(r)-4\pi r^2\rho_0^{Rh}$ for the solutions of trivalent complex salts: $[M(bpy)_3]_2(SO_4)_3$ (RCBSO) and $[M(bpy)_3]Cl_3$ (RCBCL).

and 2.6 Å, which corresponds to the longest distance between the metal atom and the contact water molecules. The distance of 6.5 Å corresponding to the bending point of $D^{Ru}(r)$ is longer than $r(Ru–H_C)$ and approximate to the distance to water molecules which may be located on the H_C atom of the bpy ligand plane. From such a consideration, the water molecules constituting the hydration shell around the $[M(bpy)_3]^{2+}$ ion are presumed to construct the network structure with a base on the periphery of $H_B(H_3, H_{3'}, H_5, H_{5'})$ and $H_C(H_4, H_{4'})$ atoms of the ligands. The distance of 8.0 Å from the metal atom of $[M(phen)_3]^{2+}$ to the center of hydration shell is equal to $\{r(Ru–H_B)+r(Ru–H_C)\}/2$ plus 2.5 Å. The intersection point between the $D^{Ru}(r)-4\pi r^2\rho_0^{Ru}$ curve of $[M(phen)_3]^{2+}$ and the abscissa is close to 8.9 Å, equal to the sum of $r(Ru–H_D)$ and 2.6 Å, which corresponds to the longest distance to the contact water molecules. Therefore, the network structure in the hydration shell of the $[M(phen)_3]^{2+}$ ion may be constructed with a base on the periphery of $H_B(H_3, H_8, H_{4a}, H_{6b})$, $H_C(H_4, H_7)$, and $H_D(H_5, H_6)$ atoms of the ligands.

In the curve of $D^{Ru}(r)-4\pi r^2\rho_0^{Ru}$ for the solutions of divalent complex salts, the second broad peak was found beyond 10 Å and was attributed to the second hydration shell sur-

rounding the first one. The centers of the second shell were located around 11.2 Å and 11.5 Å in the solutions of the $[M(bpy)_3]^{2+}$ and $[M(phen)_3]^{2+}$ complexes, respectively. These distances are by 3.5 Å longer than those for the first shell. The formation of the second hydration shell is presumed to be related to the directional hydrogen-bonded network structure in the first hydration shell: The hydrogen-bonded connections may be highly developed along the spherical surface surrounding the complex ion and reduced in the direction perpendicular to the surface.

In concentrated solutions, the hydration shells may contain not only water molecules and anions but also a part of adjacent complex ions, if considering the average distance between the complex ions, for instance, estimated to be 12.8 Å in the 0.8 M solutions of $[M(phen)_3]SO_4$, provided that the complex ion is symmetrically surrounded by six adjacent ones. This predicts that the hydration shells will become gradually disordered with increasing concentration, but the actual concentration effect is not so serious, from a comparison of the peak shapes between the 0.80 M (RNPSO(A)) and 0.26 M (RNPSO(B)) solutions of $[M(phen)_3]SO_4$. This suggests that the disordered state is practically avoided by some sharing of the hydrogen-bonded network structure between the adjacent complex ions or by the self association of the complex ions.[6)]

Hydrophobic Hydration Structure of $[M(bpy)_3]^{3+}$ (M=Rh and Cr). A small peak around 3.5—3.7 Å in the $D^{Rh}(r)$ function shown in Fig. 7a or 7b could be almost explained as a part of the feet of adjacent metal–carbon interaction peak; the difference between experimental and theoretical curves was comparable to background ripples. That is, the presence of a significant number of water molecules was not recognized within about 4.5 Å. Residual curves of $D^{Rh}(r)$ obtained by removing the metal–ligand interaction are shown in Fig. 9 for the solutions of $[M(bpy)_3]_2(SO_4)_3$ (RCBSO) and $[M(bpy)_3]Cl_3$ (RCBCL). Although some spurious peaks are involved in $D^{Rh}(r)$ for the sulfate solution because of lower concentration, the shapes of $D^{Rh}(r)$ are similar to each other, but significantly different from $D^{Ru}(r)$ for the solutions of $[M(bpy)_3]SO_4$ (RNBSO), except for the presence of a jump around 6.5 Å. Practical distribution of molecules around the trivalent complex is found to start from about 4.7 Å, with a small maximum around 5.5 Å. About one chloride ion may be present within 6 Å in the 0.73 M solutions of $[M(bpy)_3]Cl_3$, considering a=5.6 Å and K_A=28±2 dm^3 mol^{-1} at infinite dilution for the ion association between $[Co(bpy)_3]^{3+}$ and Cl^- as described above. In the crystal of $[Rh(bpy)_3]Cl_3 \cdot 4H_2O$,[35)] some chloride ions are located in the region between 4.7 and 5.9 Å. In the solutions of $[M(bpy)_3]_2(SO_4)_3$, the sulfate ion is probably not in contact with the complex ion, considering the strong hydration of sulfate ion as well as a=8.9 Å estimated for the ion association between $[Co(phen)_3]^{3+}$ and SO_4^{2-}, but one or two oxygen atoms of the sulfate ion may be located within 6 Å interposing one water molecule. However, no distinct peak reflecting the anion seems to appear in the $D^{Rh}(r)$ curves, probably because the anion, if present in the vicinity of the complex ion, is not localized at a definite position.

The analyses of $D^{Rh}(r)$ ignoring the anion distribution gave the following results as the water molecule distribution around the $[M(bpy)_3]^{3+}$ ion. The closest water molecules were located at r(Rh–H_2O)=4.73(5) Å with l=0.11 Å and n=2.9(5) in the sulfate solution (RCBSO), and at r(Rh–H_2O)=4.70(5) Å with l=0.11 Å and n=1.8(5) in the chloride solution (RCBCL). Location and number of subsequent water molecules were as follows: $n(H_2O)$=4.0 around r=5.2 Å, $n(H_2O)$=4.6 around r=5.6 Å, and $n(H_2O)$=4.0 around r=6.0 Å in the sulfate solution (RCBSO); $n(H_2O)$=3.8 around r=5.1 Å, $n(H_2O)$=5.6 around r=5.5 Å, $n(H_2O)$=4.0 around r=6.0 Å in the chloride solution (RCBCL); these structure parameters may involve some arbitrariness or uncertainties. The total numbers of water molecules ($\sum n(H_2O)$) within 6.0 Å became apparently 15.5 and 15.2 in the solutions of sulfate and chloride of $[M(bpy)_3]^{3+}$, respectively, significantly larger than 8.1 within 5.9 Å and 12.4 within 6.3 Å in the sulfate solution of $[M(bpy)_3]^{2+}$. If one chloride ion is present within 6.0 Å in the chloride solution, $\sum n(H_2O)$ is estimated to be about 13.5 by considering the difference of the scattering intensities between Cl^- and H_2O. If one or two oxygen atoms of sulfate in exist within 6.0 Å in the sulfate solution, $\sum n(H_2O)$ becomes about 14.5 or 13.5, respectively. Under the extreme condition such as infinite dilution, $\sum n(H_2O)$ in this region may be increased by one or two compared to that in concentrated solutions, since additional water molecules may come into this region instead of the anions. Anyway, it seems likely that excess water molecules of 4—6 are included within 6.0 Å around the $[M(bpy)_3]^{3+}$ ion compared to the $[M(bpy)_3]^{2+}$ ion, mostly within 5.6 Å considering the distribution intensity difference.

A large part of water molecules existing in the region of 4.7 to 6.0 Å is probably located in the vicinity of hollows along the C_3 axis of the trivalent complex, similarly to those for the divalent one. The position of excess water molecules or chloride ions in the vicinity of the complex ion may be entirely different from that of the other water molecules. In the crystal of $[Rh(bpy)_3]Cl_3 \cdot 4H_2O$,[35)] one chloride ion and one water molecule are located at 4.70 and 5.73 Å, respectively, hydrogen-bonded to each other in a hollow along the C_2 axis of the complex; the chloride ion is in contact with the C_2 atom of a bpy ligand. A similar situation is also probable in the solution: for instance, excess water molecules or chloride ions may exist in the three hollows along the C_2 axes in the region of 4.7 to 5.6 Å from the metal atom. The volume of vacant space in these hollows is presumed to be closely related to the degree of hydrophobicity of the complex ion. The penetration of some water molecules or anions into the space in the case of the trivalent complex ion is caused by the increase of the electrostatic attraction force dependent on the ionic charge, and results in some reductions of the volume of the vacant space as well as of the degree of the hydrophobicity. The difference (28 cm^3 mol^{-1}) in V^∞(ion) between $[Ru(bpy)_3]^{2+}$ and $[Rh(bpy)_3]^{3+}$ (Table 2) is related to this volume reduction which is partially compensated by the expansion effect due to the decrease of molecular density

in the hydrophobic hydration shell as described below.

A broad peak corresponding to the first hydrophobic hydration shell around the trivalent complex ion is found in the $D^{Rh}(r)-4\pi r^2\rho_0^{Rh}$ curves shown in Fig. 10 (RCBSO and RCBCL). The center of the hydration shell is located around 7.7 Å in the solutions of sulfate (RCBSO) and chloride (RCBCL) of $[M(bpy)_3]^{3+}$, in agreement with the distance observed for the solutions of $[M(bpy)_3]SO_4$ (RNBSO); the thicknesses of the shell are also similar to each other for the divalent and trivalent complexes. However, the peak is recognized to sink as a whole, indicating the reduction of molecular density caused by the decrease of the number of molecules in the hydration shell. Further, the second broad peak corresponding to the second hydration shell is not observed for the trivalent complex ions. These phenomena suggest the reduction of the hydrophobicity of the complex ion as predicted from the ionic charge dependence of temperature coefficients of the Walden product.

The authors thank Professors Hitoshi Ohtaki (Ritsumeikan University), Hisanobu Wakita (Fukuoka University), Toshio Yamaguchi (Fukuoka University), Kazuhiko Ozutumi (Ritsumeikan University), Georg Johansson (Royal Institute of Technology), and Magnus Sandström (Royal Institute of Technology) for their helpful suggestions about the X-ray diffraction measurements. The authors also thank Professors Satoshi Tachiyashiki (Kagawa Nutrition University) and Yuichi Masuda (Ochanomizu University) for their useful discussions.

References

1) K. Miyoshi, Y. Kuroda, J. Takeda, H. Yoneda, and I. Takagi, *Inorg. Chem.*, **18**, 1425 (1979).
2) S. Tachiyashiki and H. Yamatera, *Bull. Chem. Soc. Jpn.*, **55**, 759 (1982); *Inorg. Chem.*, **25**, 3209 (1979).
3) A. Yamagishi, *J. Phys. Chem.*, **86**, 2472 (1982).
4) J. K. Barton, J. J. Dannenberg, and A. L. Raphael, *J. Am. Chem. Soc.*, **104**, 4967 (1982).
5) T. Fujiwara, E. Iwamoto, and Y. Yamamoto, *Inorg. Chem.*, **23**, 115 (1984).
6) Y. Masuda and H. Yamatera, *Bull. Chem. Soc. Jpn.*, **57**, 58 (1984); *J. Phys. Chem.*, **88**, 3425 (1984).
7) T. Tominaga, S. Matsumoto, T. Koshiba, and Y. Yamamoto, *Chem. Lett.*, **1988**, 1427.
8) H. Yokoyama, Y. Koyama, and Y. Masuda, *Chem. Lett.*, **1988**, 1453.
9) H. Yokoyama, K. Shinozaki, S. Hattori, F. Miyazaki, and M. Goto, *J. Mol. Liq.*, **65/66**, 357 (1995).
10) H. Ohtaki and T. Radnai, *Chem. Rev.*, **93**, 1157 (1993).
11) G. Johansson and H. Yokoyama, *Inorg. Chem.*, **29**, 2460 (1990).
12) H. Yokoyama and G. Johansson, *Acta Chem. Scand.*, **44**, 567 (1990).
13) G. Johansson, H. Yokoyama, and H. Ohtaki, *J. Solution Chem.*, **20**, 859 (1991).
14) H. Yokoyama, S. Suzuki, M. Goto, K. Shinozaki, Y. Abe, and S. Ishiguro, *Z. Naturforsch., A*, **50a**, 301 (1995).
15) K. Shinozaki, K. Miwa, H. Yokoyama, and H. Matsuzawa, *J. Chem. Soc., Faraday Trans.*, **92**, 1935 (1996).
16) M. Kanakubo, H. Ikeuchi, G. P. Satô, and H. Yokoyama, *J. Phys. Chem., B*, **101**, 3827 (1997).
17) H. Yokoyama and H. Yamatera, *Bull. Chem. Soc. Jpn.*, **48**, 2708 (1975).
18) F. P. Dwyer, J. E. Humpoletz, and R. S. Nyholm, *J. Proc. R. Soc. (N. S. Wales)*, **80**, 212 (1946).
19) G. B. Kauffman and L. T. Takahashi, "Inorganic Synthesis," ed by H. F. Holtzclaw, McGraw-Hill, New York (1966), Vol. 8, p. 227.
20) C. M. Harris and E. D. Mckenzie, *J. Inorg. Nucl. Chem.*, **25**, 171 (1963).
21) M. Mori, *Nippon Kagaku Zasshi*, **74**, 253 (1953).
22) H. Yokoyama and T. Ohta, *Bull. Chem. Soc. Jpn.*, **61**, 3073 (1988).
23) H. Yokoyama and H. Kon, *J. Phys. Chem.*, **95**, 8956 (1991).
24) H. Yokoyama and T. Ohta, *Bull. Chem. Soc. Jpn.*, **62**, 345 (1989).
25) H. Yokoyama, M. Mochida, and Y. Koyama, *Bull. Chem. Soc. Jpn.*, **61**, 3445 (1988).
26) H. Yokoyama and H. Yamatera, *Bull. Chem. Soc. Jpn.*, **48**, 1770, 3002 (1975).
27) Unpublished data.
28) R. L. Kay, "Ionic Transport in Water and Mixed Aqueous Solvents," in "Water," ed by F. Franks, Plenum, New York (1973), Vol. 3, Chap. 4.
29) M. Yasuda, *Bull. Chem. Soc. Jpn.*, **41**, 139 (1968).
30) H. Ichida and S. Tachiyashiki, "the 39th Symposium on Coordination Chemistry of Japan," Mito, September 1989, Abstr., No. 3BP11, and private communication.
31) K. R. Butler and M. R. Snow, *J. Chem. Soc. A.*, **1971**, 565.
32) D. P. Rillema, D. S. Jones, and H. A. Levy, *J. Chem. Soc., Chem. Commun.*, **1979**, 849.
33) H. Tamura, N. Ikeda, T. Iguro, T. Ohno, and G. -E. Matsubayashi, *Acta Crystallogr., Sect. C*, **C52**, 1394 (1996).
34) A. Wada, N. Sakabe, and J. Tanaka, *Acta Crystallogr., Sect. B*, **B32**, 1121 (1976).
35) B. Hubesch, B. Mahieu, and J. Meunier-Piret, *Bull. Soc. Chim. Belg.*, **94**, 685 (1985).
36) K. V. Goodwin, W. T. Pennington, and J. D. Petersen, *Inorg. Chem.*, **28**, 2016 (1989).